Mitigation Options to Reduce Peak Air Temperature and Air-Conditioning Demand in the Context of a Warming Climate for a Tropical Coastal City

Rabindra Pokhrel
Department of Mechanical Engineering,
The City College of New York,
New York, NY 10031
e-mail: rabindra@ku.edu.np

Jorge E. González-Cruz
Presidential Professor NOAA-CREST,
Professor of Mechanical Engineering,
Department of Mechanical Engineering,
The City College of New York,
New York, NY 10031
e-mail: jgonzalezcruz@ccny.cuny.edu

Air conditioning (AC) demand has recently grown to about 10% of total electricity globally, and the International Energy Agency (IEA) predicts that the cooling requirement for buildings globally increases by three-fold by 2050 without additional policy interventions. The impacts of these increases for energy demand for human comfort are more pronounced in tropical coastal areas due to the high temperatures and humidity and their limited energy resources. One of those regions is the Caribbean, where building energy demands often exceed 50% of the total electricity, and this demand is projected to increase due to a warming climate. The interconnection between the built environment and the local environment introduces the challenge to find new approaches to explore future energy demand changes and the role of mitigation measures to curb the increasing demands for vulnerable tropical coastal cities due to climate change. This study presents mid-of-century and end-of-century cooling demand projections along with demand alleviation measures for the San Juan Metropolitan Area in the Caribbean Island of Puerto Rico using a high-resolution configuration of the Weather Research and Forecasting (WRF) model coupled with Building Energy Model (BEM) forced by bias-corrected Community Earth Systems Model (CESM1) global simulations. The World Urban Database Access Portal Tool (WUDAPT) Land Class Zones (LCZs) bridge the gap required by BEM for their morphology and urban parameters. MODIS land covers land use is depicted for all-natural classes. The baseline historical period of 2008–2012 is compared with climate and energy projections in addition to energy mitigation options. Energy mitigation options explored include the integration of solar power in buildings, the use of white roofs, and high-efficiency heating, ventilation, and air conditioning (HVAC) systems. The impact of climate change is simulated to increase minimum temperatures at the same rate as maximum temperatures. However, the maximum temperatures are projected to rise by 1–1.5 °C and 2 °C for mid- and end-of-century, respectively, increasing peak AC demand by 12.5% and 25%, correspondingly. However, the explored mitigation options surpass both increases in temperature and AC demand. The AC demand reduction potential with energy mitigation options for 2050 and 2100 decreases the need by 13% and 1.5% with the historical periods. Overall, the demand reduction potential varies with LCZs showing a high reduction potential for sparsely built (32%), and low for compact low rise (21%) for the mid-of-century period compared with the same period without mitigation options.
[DOI: 10.1115/1.4051160]

Keywords: air conditioning, efficiency, environment, interactive buildings, smart cities, thermal comfort

1 Introduction

The International Energy Agency (IEA) declared the rapid growth of electricity demand from building air conditioning (AC) as one of the most critical and often overlooked energy issues of our time [1]. The demand for cooling has recently grown to about 10% of total electricity globally. The IEA predicts that energy for cooling of buildings will account for 30% of the total demand by 2050 without additional policy interventions beyond the 2015 United Nations Paris Agreement. A common factor for most tropical coastal cities, where AC demand can often exceed 50% on the total energy budget [2], can be directly impacted by a changing climate.

In one of qualitative studies, Caribbean islanders described their personal experiences and perceptions about climate change as increased average temperatures, the severity of weather events, and changes in rainfall patterns [3]. Caribbean sea surface temperature is observed to be increasing [4] and so is the extreme heatwave events [5], which, in tropical and subtropical regions, will tend to increase the peak energy demands for air conditioning putting both the energy infrastructure and vulnerable population at high health risks. The medium global CO_2 emission scenario (representative concentration pathway (RCP) 4.5), which projects rising radiative forcing, reaching 4.5 W/m^2 by the end-of-the-century, may increase energy demand between 31 and 62.5% of the current climate for the Caribbean region. This increase has been projected to be a cooling peak energy demand of 8.15 GW for the Caribbean as derived from a multi-model ensemble [6]. Analysis done with higher resolution downscaling for New York city with "business

Manuscript received December 30, 2020; final manuscript received April 10, 2021; published online May 26, 2021. Assoc. Editor: Shiguang Miao.

as usual" (RCP 8.5) scenario predicts a significantly higher maximum total peak cooling demand of 3.65 GW by the end-of-century, an increase of 27.3% over the historical period of 2006–2010 [7]. Results on suburban Melbourne, Australia, located in a temperate/oceanic climatic region in which more energy currently are used to heat buildings rather than cooling, are simulated to decrease the gas demand (mainly used for heating) by 22% and increase in peak electricity demand (mainly used for cooling) by 84.5% by the end-of-century. The study considers tripling the number of AC ownerships by the end-of-21st-century [8]. Some of these studies concern particular states or regions, and the impacts estimated depend crucially on local conditions. A common question for planners, utility operators, and energy service providers is the projection of additional generation capacity required to meet the future energy demands.

Consequently, policies and programs addressing mitigation are rapidly growing in Latin America and the Caribbean [9,10]. The United Nations Environmental Program (UNEP), through its Economic Commission for Latin America and the Caribbean studies (ECLAC), has demonstrated that renewable energy sources would play an essential role in these regions contributing to improving the inhabitant's quality of life. UNEP and the World Bank have several projects dealing with mitigating climate change (by reducing energy consumptions) in regional areas, where the reduction of total electricity demand by 31% can be achieved by only improving the efficiency of appliances and heating, ventilation, and air conditioning (HVAC) equipment, and utilizing renewable energy resources like solar and wind [9]. There has also been a great deal of work on efficient building design to reduce energy loads, and the applications would differ based on specific geographic locations or the building sector [11]. High annual energy savings in building levels can be achieved by passive design [12], better thermal insulation [13], improved ventilation [14], improved efficiency of equipment and technology [2], increasing indoor cooling set-points [15], use of white or green roofs [16] among others. Aggressive policies aimed at upgrading only heating/cooling systems and appliances could result in decreased electricity use as low by 28%, potentially avoiding the installation of new generation capacity [17].

The integration of energy technologies should consider supporting the shift to sustainable generation for urban and optimum energy planning [11]. A recent study highlights that the built environment of the future would transform buildings into resource assets-fully self-aware, adaptive, and a two-way communication with the electric grid (to optimize operating cost) that add market value to the assets [18]. In addition to this, the stricter de-carbonization regulation would open doors to innovative designs and renewable energy integration in all building sectors. The free space available on rooftops can be used with full potential for energy services to achieve the de-carbonization goals and increase the building value. For city-scale deployment, different types of roof applications (cool roof, green roof, and photovoltaic (PV) roof) on buildings have shown to reduce air temperatures and energy consumptions [19–24]. One such means is rooftop PV installations, which shows to decrease the temperature and urban heat island (UHI) effects [19,25] especially reducing day time UHI and peak energy demands [26]. It shows that a higher albedo of a tilted PV shaded roof can act as a radiant barrier that reflects thermal radiation from the roof surface [27]. Radiant barriers have widely used to reduce radiant heat transfer from the roof to building which recently has been promoted by US DOE and Florida Solar Energy Center (FSEC).

In this work, we evaluate mitigation options (a combination of cool roof, titled PV, and efficient HVAC systems) based on the recommendations for reducing peak demands (with a reduction potential of 33%) from earlier studies by Pokhrel et al. [26,28] for San Juan Metropolitan Area (SJMA) of Puerto Rico. This study may also support public energy policy such as the Puerto Rico Integrated Energy Resource Plan (IRP) which aims to increase energy efficiency in the island by 25% by 2030, and the integration of renewable energy resources by 100% by 2050 [29].

The evaluation of energy demands at larger urban scales has either focused on the use of statistical [30,31] or process-based models [32,33]. The absence of interaction between weather and building is one of the limitations of these approaches and could amplify in the context of changing climate. An approach to resolve this limitation is by coupling weather prediction to Building Energy Models (BEMs) [7,34,35]. However, the computation cost and lack of urban morphology and its corresponding parameters have limited the studies to a few events or in cases to short periods (<1 season). Here, we present the impacts of climate change and energy mitigation measures on 2-m air temperature and cooling energy demand reduction potential for the dense population region of SJMA for an extreme emission scenario for a multi-year period. The impact of climate change is compared with historic periods (2008–2012) for late rainfall seasons (LRSs) (August to November) of the San Juan Metropolitan region of Puerto Rico for both mid (2048–2052) and end centuries (2092–2096). Similar work has been reported for New York City (NYC) where peak air conditioning demand is expected to rise by 27% by end-of-century periods under the RCP 8.5 scenario [7]. However, the impacts of different energy mitigation measures to combat extreme heat and peak air conditioning demand become as important as the impacts of climate change alone. Also, cities around the world are exploring cool roofs, solar PV, and energy efficiency measures to reduce the carbon footprints as well as improve grid resiliency. Besides, understanding of potential energy demand reduction measures, which can serve as indispensable information for the end-users, the projection of energy demand can also help to delineate areas (or regions) where high reduction potential can occur and could serve as a guide for future recommendations and policies. Recommendations for a combination of building-integrated energy mitigation measures such as cool roof, higher coefficient of performance (COP) HVAC systems, and titled solar PV are based on past works done by Pokhrel et al. 2020 [26,28] where each individual option was assessed. Here, we assess the combination of all energy mitigation options under long-term climate projections.

2 Methods

2.1 Simulation Setup. The flowchart shown in Fig. 1 describes this study's overall methodology. We use a high-resolution configuration of the Weather Research and Forecast (WRF) model [36] coupled with a modified multi-layer urban canopy and BEM parametrization as a tool to study changes in building cooling demand under climate change conditions. The bias-corrected runs of the Community Earth Systems Model version 1 (CESM1) [37] datasets are used as initial and boundary conditions. The regional-scale biases due to having coarse spatial resolution and limited representation of some physical processes are corrected in CESM1 with the bias correction method developed by Skamarock et al. [36]. Their work adjusts CESM outputs by combining a 25-year (1981–2005) mean annual cycle from ERA-Interim reanalysis and a 6-hourly perturbation period representing the climate signal. The bias correction removes the mean annual bias while retaining the day-to-day climate variability from CESM as follows:

$$\mathrm{CESM_{BC}} = \mathrm{ERAI(mean)} + \mathrm{CESM'}$$

Regional modeling forced with bias-corrected CESM was shown to improve results for the North Atlantic and the North America [38]. Specifically, temperature over the Caribbean region showed a decreased cold bias when all boundary condition variables were corrected with reanalysis data. Sea surface temperature from bias-corrected CESM is updated daily.

Since this study concerns peak energy demand for a tropical coastal city, urban morphology (land cover land use (LCLU)) and

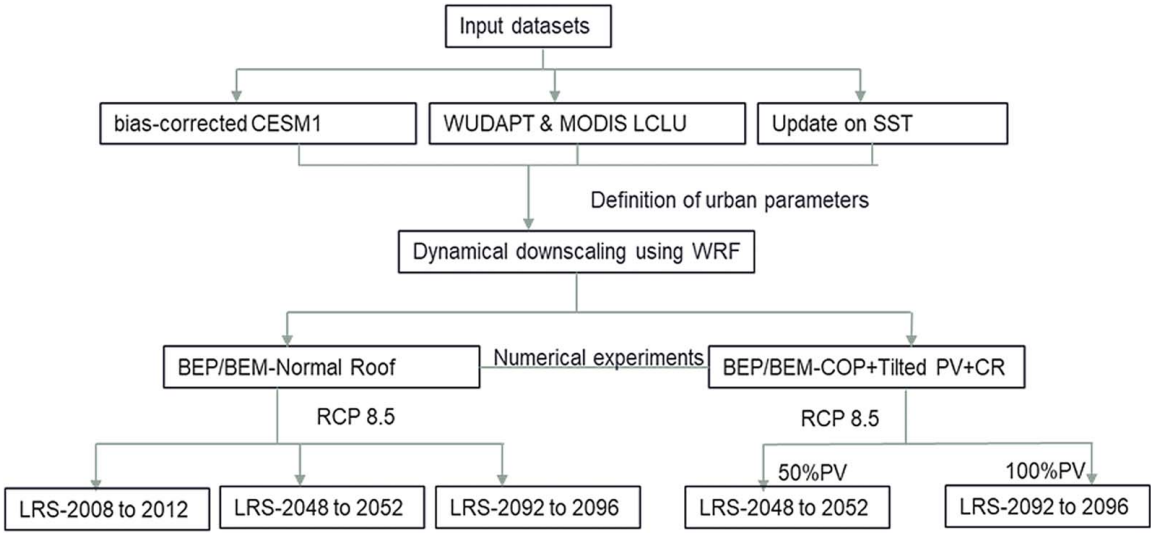

Fig. 1 The overall methodology adopted in this study

urban parameters (provided by a look-up table) become an essential component in urban canopy models like building effect parameterization (BEP) and BEM, which provides momentum and energy exchange with the atmosphere. For major US cities, National Urban Database and Access Portal Tool (NUDAPT) [39] is typically used for defining urban morphology and its corresponding parameters in urban physics parameterization. Limitations of NUDAPT classification for Puerto Rico led us to use World Urban Database Access Portal Tool (WUDAPT) Land Class Zones (LCZs) [40]. For this work, we use the WUDAPT LCZs for the SJMA of Puerto Rico, which has been validated with LANDSAT 8 imagery for surface albedo by an earlier study [26].

The smallest domain of urbanized WRF was set up to run at a finer spatial resolution of 1 km over the eastern region of SJMA. Two nested domains of 5 km and 25 km resolution parent domain consist of a larger area to capture synoptic conditions consisting of countries of Mesoamerican and the Caribbean region and the surrounding ocean. For planetary boundary level 50 vertical levels 35 of which are below 2 km height are used in the atmospheric component with a time-step of 45 s for the coarsest domain, and each nested domain has three-time-steps per parent domain calculation.

The model parameterization used follows the past work done [7,26] and is tabulated in Table 1.

2.2 Numerical Experiments. Peak 2-m-air temperature and energy demands for Puerto Rico occur during the LRS covering August to November. During LRS, both extreme temperature events and peak energy demands exist for the entire island [49]. In this study, simulations are evaluated only for five LRSs, from 2008 to 2012 (considered as historic or current), from 2048 to 2052 (considered as mid-century), and from 2092 to 2096 (considered as end-of-century) to capture LRS variability of current, mid-century, and end-century period, respectively. We consider a worst-case projection based on RCPs [50] a "business as usual" (RCP 8.5) scenario, which projects rising radiative forcing, reaching 8.5 W/m^2 by the end-of-the-century. The simulation covers two sets of experiments: normal conditions and mitigation alternatives. The normal condition represents normal roof conditions as in BEM, and mitigation alternatives covers building-integrated passive systems such as cool roof (albedo changed to 70% for each LCZ from its normal value in the urban parameterization look-up table; Table 3), and active systems such as higher COP (for each LCZ is changed to 3.5 from 3, provided in Table 3), and tilted solar PV in roofs (50% of roof area for mid-of-century and 100% of roof area for end-of-century) based on their reduction potential for the same region. The passive building-integrated mitigation options considered here have been previously studied [26]. For a roof with tilted PV, the approach follows a recent study by Pokhrel et al. [26] where the building roof temperature of BEM has been adjusted using modifications based on the energy balance of roof including tilted PV. Table 2 presents both building parameters and AC input parameters used in BEM for each LCZ. The input building parameters include details of building properties, whereas AC parameters include loads from people, equipment, and operational schedules. The key parameters with their corresponding values used in this work are gathered from different sources [26,28,39,51–53]. The impacts of individual mitigation measures are discussed in detail in previous work by Pokhrel et al. [26,28] for short-term periods; however for longer periods, the impact of individual mitigation measures would require expensive computation resources. For this reason, we adapted the combination of the mitigation measures: cool roof, efficient HVAC systems, and solar PV (tilted) to study its combined role for long-term projections. Besides the combined reduction potential, these mitigation measures are chosen based on the Puerto Rico Energy Bureau report (IRP, PREPA 2019),[1] where Puerto Rico passed a public policy bill to increase efficiency measures by 40% and installed renewable generation to 100% by 2050. All numerical experiments assessed were based on static land surface morphology similar to the reference period of 2008–2012, which consists of WUDAPT LCZs for urban classes and MODIS LCLU for natural classes. WRF region of interest with a two-way nesting domain is plotting in Fig. 2 with a coarser domain at 25 km and a finer domain at 1 km resolution where the LCZs for urban classes and MODIS LCLU are shown in Fig. 2 for the finer domain of 1 km.

Table 1 Model physics parameterizations used in WRF simulations

Model physics	Parameterization
Land surface model	NOAH LSM [41]
Cumulus	Kain–Fritsch (off in D03) [42]
Microphysics	WSM 6 [43]
Urban canopy	BEP [44]
	BEM [45]
Shortwave radiation	Dudhia [46]
Longwave radiation	RRTM [47]
Planetary boundary layer (PBL) scheme	Mellor–Yamada–Janjic (MYJ) [48]

[1]https://www.edf.org/media/puerto-ricos-irp

Table 2 Daily electricity air conditioning demand (observed and simulated) for SJMA in GW-h for late rainfall seasons

Periods/LCZ	Compact high rise	Compact mid rise	Compact low rise	Open low rise	Sparsely built	Total	% change
2010 (observed)						8.960	
2010	1.393	0.450	7.850	0.624	0.500	10.815	N/A
2050	1.530	0.501	8.824	0.717	0.574	12.145	12.298
2050 + options	1.234	0.400	6.798	0.541	0.433	9.405	−13.042
2100	1.681	0.556	9.907	0.819	0.655	13.617	25.906
2100 + options	1.361	0.446	7.717	0.627	0.501	10.652	−1.520

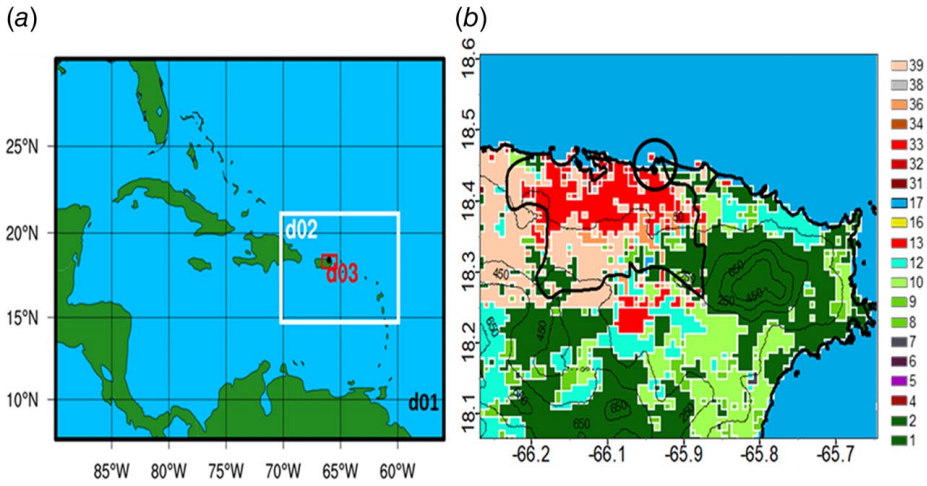

Fig. 2 (*a*) WRF simulation domain and (*b*) WUDAPT + MODIS derived land use index inside D03 with elevation contours. MODIS LCLU of 2, evergreen broadleaf forest; 8, woody savannas; 9, savannas; 10, grasslands; 12, croplands; 17, water and WUDAPT LCZs; 31, compact high rise; 32, compact mid rise; 33, compact low rise; 34, open high rise; 36, open low rise; 38, large low rise; and 39, sparsely built. The black dot inside the circle in (*b*) represents the location of SJIA.

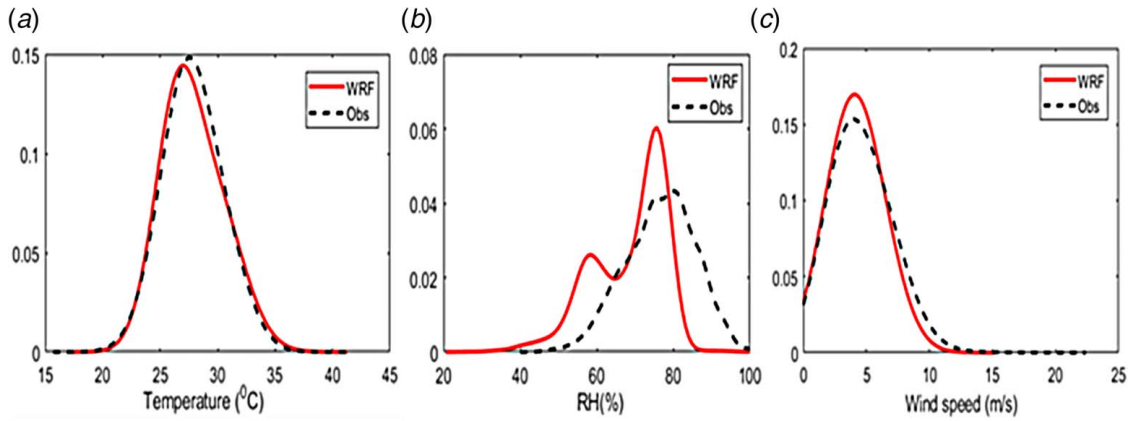

Fig. 3 Kernel density estimates of (*a*) daily maximum temperature, (*b*) relative humidity, and (c) wind for historical simulation period (2008–2012) for every LRS for observations and WRF simulation

3 Results

3.1 Model Evaluation. Historical period simulations are evaluated against the San Juan International Airport (SJIA) station for daily maximum temperature, relative humidity, and wind speed (Fig. 3). Simulated results compared against Kernel density estimates (KDEs), an approximation of a dataset's distribution. The airport station reported a mean daily maximum of 27.6 °C with a standard deviation of 3.59 °C. WRF simulations result, interpolated using nearest neighbor, showed a mean daily maximum of 26.9 °C (2.5% error) with 3.84 °C standard deviation (7% error). These results are consistent with Ortiz et al. [7] for New York city, which found less than 1% and 10% error on the mean of daily maximum temperatures and standard deviation, respectively. Relative humidity, in general, is underestimated in the WRF simulation for values less than 40% and higher than 80%. The bimodal nature of the relative humidity is observed in the weather station at 73 and 82%. The bimodal nature is also captured in WRF simulation at 57 and 73%. Wind speed for both observation and simulation has a mean of 4.8 m/s; however, the maximum wind speed is underestimated by the simulation for values higher than 8 m/s by 1–1.5 m/s. The simulated maximum wind speed of 15 m/s compares

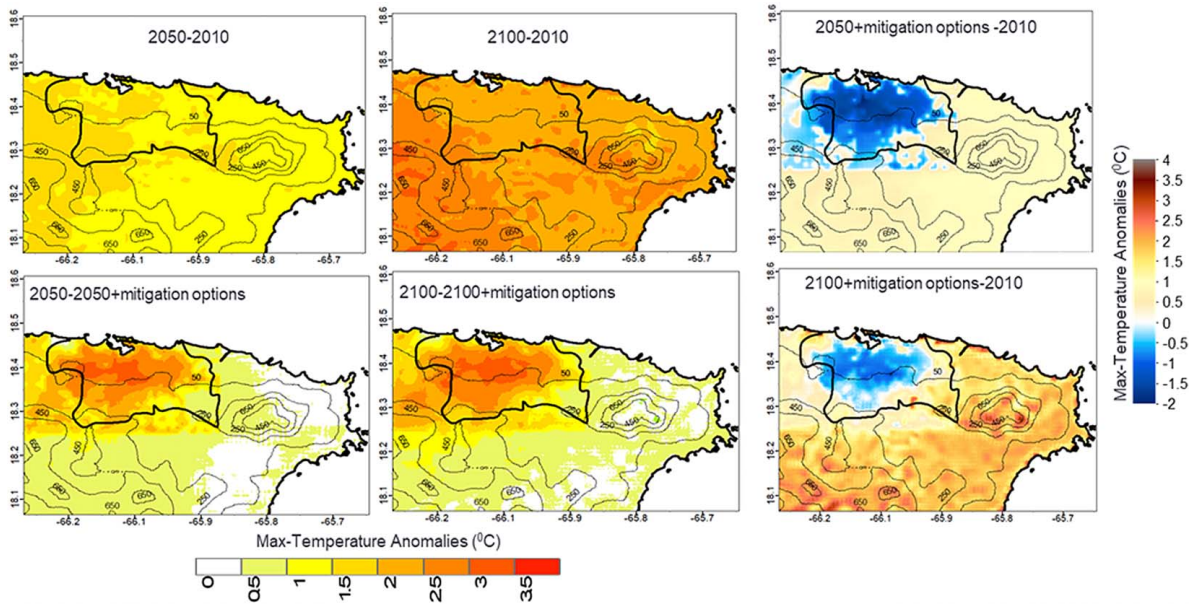

Fig. 4 Mean of peak temperature anomalies [$T_{max(2050)}-T_{max(2010)}$] for mid-of-century (2050) and end-of-century [$T_{max(2100)}-T_{max(2010)}$] (2100) without mitigation options and with mitigation options (2050+mitigation options-2010)

with 23 m/s with observation. Overall, we consider this validation of the simulated environmental variables reasonable acceptable for the purpose of this study.

3.2 Spatial Temperature and Cooling Load Projections. Peak temperature projections are presented as anomalies increase or decrease over the historical period of 2008–2012 over the mid- and end-of-century (Fig. 4). The anomalies for 2050 and 2100 show an increase of peak temperature by 1–1.5 °C and 2.5 °C, respectively, for the delineated San Juan Metropolitan region. The increase in temperature is uniform for the urban region as well as for natural land cover. The mitigation options adopted here reflect maximum changes in the urban area representing cooling effects,

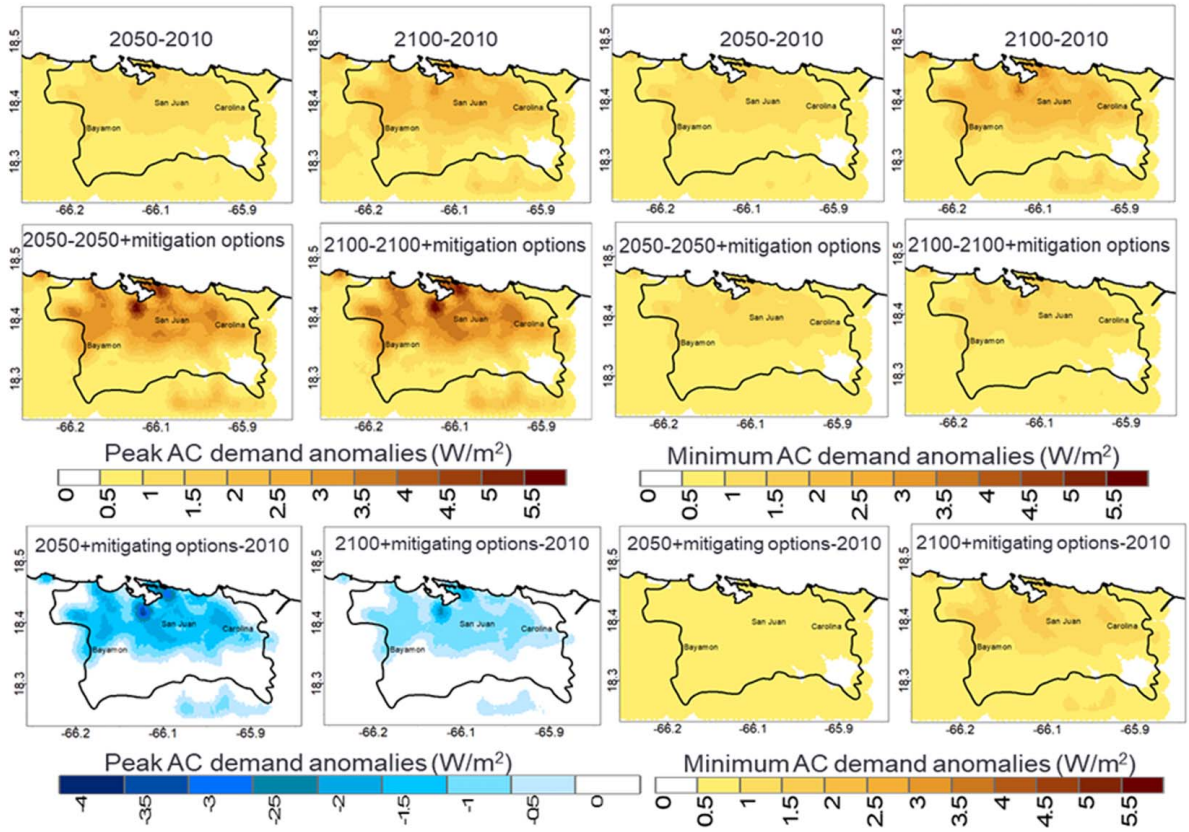

Fig. 5 Peak AC peak demand anomalies for mid-of-century (2050–2010) and end-of-century (2100–2010) without mitigation options and with mitigation options (2050+mitigation options-2010 and 2100+mitigation options-2010) as shown in left panel. The right panel shows minimum AC demand anomalies accordingly.

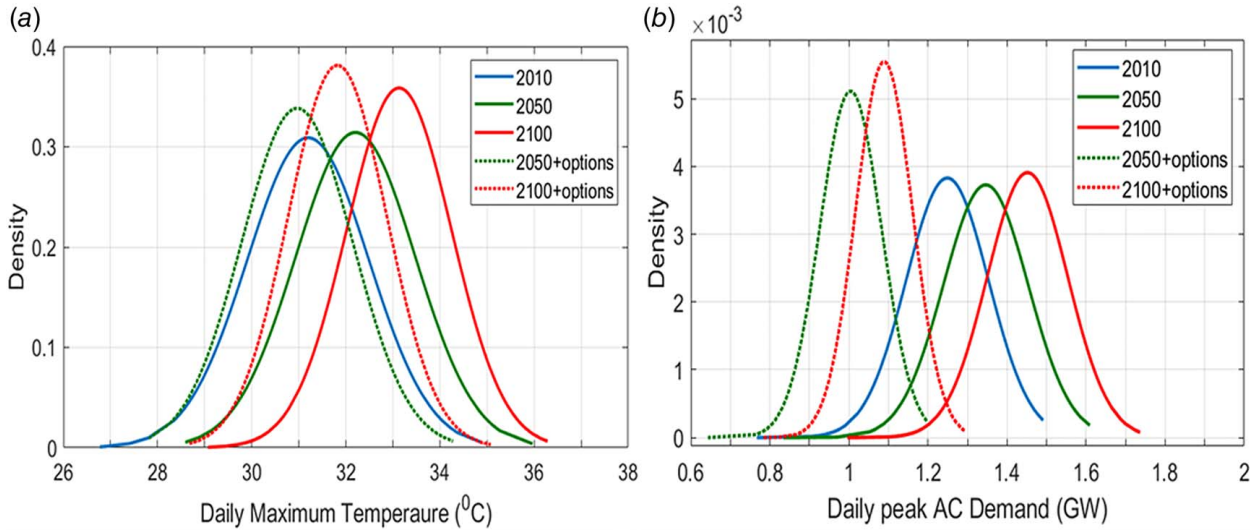

Fig. 6 Probability density function (PDF) of (*a*) mean daily maximum temperature and (*b*) mean peak AC demand for densely packed region of SJMA

whereas the non-urban locations show a similar increase as of 2050 and 2100. The cooling effects are lower than −0.5 °C for 2100 and as high as −2 °C for 2050 in SJMA. The reduction potential of maximum temperatures by 2050 is much higher than in 2100, as expected. The results presented help understand the impacts of mitigation options under the warming climate of 2050 and 2100. For 2050 and 2100, the mitigation options reduce the urban temperature by 2.5–3 °C as compared to without mitigation options for the same period. The results show that the reduction potential is much higher than the increase in both mid- and end-of-century temperatures. Climate change impacts simulated to increase minimum temperatures (not shown) at the same rate as maximum temperatures; however, the mitigation options proposed here have a small reduction potential as compared with peak temperatures.

The increase in maximum and minimum AC demands is presented as anomalies with respect to the historical period (Fig. 5). The spatial distribution of the increase of peak AC demand per municipality is an essential metric for utilities as it is indispensable for the planning of generation and transmission resources. Besides, the mitigation options (a combination of cool roof, tilted PV, and higher COP HVAC equipment) highlight the regions where maximum demand reduction potential can be achieved. The peak AC demand increase for 2050 and 2100 is 1.5 W/m^2 and 3 W/m^2, respectively, for San Juan municipality, which represents an increase of peak demand by 12.5% and 25%, respectively. The minimum anomalies simulated present an increase by the same amount, however, have a much higher reduction potential of 21% and 35% for 2050 and 2100, respectively. For the mid- and end-century reduction potential, mitigation options are much higher by 3.5–4 W/m^2, surpassing the increase of 1.5–3 W/m^2 for the same period as shown by maximum anomalies (Fig. 5). Mid-of-a-century and end-of-century mitigation options reduce the minimum AC demand by 1 W/m^2. Urban cooling reflected in 2050 with combined mitigation options for peak AC demand anomalies of −3 W/m^2; however, it reduces to −1.5 W/m^2 for 2100. The mitigation options for minimum AC demand for 2050 and 2100 are not enough to meet the new increased AC demand for the same period. The mitigation options, however, show a cooling effect of reducing the peak AC demand by 2 W/m^2 for peak demand, whereas the minimum AC demand reduces by 0.5–1 W/m^2 as compared with the historical period.

3.3 Mean Maximum Temperature and Total AC Demand.

In addition to the spatial distributions of temperatures and peak AC demands, the peak temperatures and peak AC demands projections for the entire metropolitan region are relevant indicators for weather services and utility managers as they may serve for the planning of mitigation and generation and transmission resources for the future. Herein, we present probability density functions for three climate periods with and without mitigation options (a combination of cool roof, tilted PV, and higher COP HVAC equipment) (Fig. 6). Daily maximum temperatures (in °C) for the entire high-density region in SJMA have mean values at 31.2, 32.2, and 33.2 °C for 2010, 2050, and 2100, whereas the mitigation options reduce them to 31.0 and 31.8 °C for 2050 and 2100, respectively. The mitigation measures reduce the maximum temperature threshold of extreme hot events of San Juan (where maximum daily temperature is between 30.1 and 35.0 °C, representing 86–99 percentile and 32.2 °C threshold as 90 percentiles [47,54]) as shown in Fig. 6(*a*). The tail of the peak AC demand (in GW) for the same region with mean at 1.49, 1.61 (8% increase), and 1.72 (16% increase) for 2010, 2050, and 2100, whereas the mitigation options reduce it to 1.2 (decrease of 20%) and 1.295 GW (13%) for 2050 and 2100 as compared with 2010. The reduction potential for 2050 and 2100 as compared to without mitigation adaptation decreases the peak by 25%.

The combination of mitigation options (cool roof, tilted PV, and efficient HVAC system) has a high reduction potential that varies with each LCZ in the metropolitan region. The total daily demand is compared with monthly observation records for the entire island using data from the Puerto Rico Electric Power Authority[2] for the historic period of the LRS covering the years of 2008–2012. Electric energy per capital is first calculated from the record and is multiplied by total population of SJMA for 2010.[3] It is assumed that most of the energy used in the residential and commercial sectors is in air conditioning to maintain human comfort in the buildings sector [55], a common factor for most tropical coastal cities, where air conditioning can often exceed 50% on the total energy budget [2]. Thus, the total electricity consumption is factored by 60% to account for electricity consumption by the air conditioning system for SJMA. The resulting daily for the historic period of 2010 (which is the average of daily demands for LRS for 2008–2012) is presented as observation in Table 2. The present-day BEP + BEM scheme assumes that all spaces inside the buildings undergo air conditioning, but it is a fact that some indoor spaces are not cooled and some buildings are not even equipped with AC systems. To represent this reality, the building area fraction as a function of LCZ classes is thus introduced which is a

[2]https://aeepr.com/en-us
[3]https://www.census.gov/

product of building area fraction and conditioned fraction. For compact high rise, compact midrise, compact low rise, open low rise, and sparsely built region, the building area fraction is tabulated in Table 3, whereas the conditioned fraction of 0.5 for all urban LCZs is used. These products are then used for every grid cells (1 km by 1 km^2) in SJMA to compute the total electrical AC demands. These methods are consistent with a total conditioned fraction of 50%, close to previous studies for example, 60% for Tokyo [56] and Madrid [57] and 65% for Phoenix [58] and 50–60% for urban classes of Xu et al. [59]. The summary of mean daily AC demand for each LCZ for the entire densely packed region of SJMA (Table 2) shows the increase of AC demand by 12.3% and 26% for mid-of-century and end-of-century as compared with 2010. The demand increase varies with LCZs. For example, the increase in demand for LCZ39 (sparsely built) for 2100 as compared with 2010 is 32%, whereas, for LCZ31, the increase is 21%. The reduction potential with and without adaptation of mitigation options for 2100 for the same LCZs is 24% and 19%, respectively. The difference in demand and reduction potential with mitigation adaptation can serve as an asset for the utility company and energy providers to delineate areas where high reduction potential occurs. There is a 20% over estimation for daily electric AC demand for simulation as compared with the observed utility record for current climate (2010), as tabulated in Table 2. This is mainly due to the assumption of 100% AC ownership at SJMA.

4 Conclusions and Future Work

Tropical coastal cities are at higher risks of increasing temperatures due to global warming for the compounded effects of an uncomfortable environment and increases in building energy demands to mitigate warmer and humid conditions. The Caribbean is one of those regions where building energy demands often exceed 50% of the total electricity demand and is projected to increase due to the warming climate. In this study, we project future energy demand changes and the role of mitigation measures to curb the increases in energy demands for vulnerable tropical coastal cities due to climate change. This study presents mid-of-century and end-of-century cooling demand projections along with demand alleviation measures for the case of the San Juan Metropolitan Area of Puerto Rico using a high-resolution configuration of the Weather Research and Forecasting model coupled with BEM. Increases of maximum temperatures are projected to rise by1–1.5 °C and 2 °C for mid- and end-of-century, respectively, consequently increasing peak AC demand by 12.5 and 25%, respectively. Mitigation options explored considered a combination of cool roof, higher COP for AC, and use of building-integrated solar PV panels, surpasses both increases in temperature and AC demand. The AC demand reduction potential with mitigation options for 2050 and 2100 decreases peak demand by 13% (1.41 GW) and 1.5% (0.163 GW) from the historical periods (of about 10.815 GW). The demand reduction potential varies with LCZs showing high reduction potential for the sparsely built region (32%) and low for compact, low rise (21%) for a mid-of-century period as compared with the same period without mitigation options. Also, the daily maximum temperatures (in °C) for the high-density region of SJMA have mean at 31.2, 32.2, and 33.2 for 2010, 2050, and 2100, whereas the mitigation options reduce it to 31.0 and 31.8 for 2050 and 2100, respectively. For 2050 and 2100, the mitigation options reduce the urban temperature by 2.5–3.0 °C as compared with without mitigation options. The projection of peak and total cooling demand may be similar for other tropical coastal cities, although the magnitude would be different depending on the size, form, and function of the urban coverage.

We outline some limitations of the study and possible areas for future improvements. The proposed mitigation options reduce peak temperatures and AC demands; however, the increase of AC ownership may also depend on the rise of warmer mean temperatures [60]. BEM outputs take into account 100% AC ownership for each LCZ. Our assumption of 50% AC ownership could be improved with actual data from the local utility. Other limitations like assumptions of historic LCLU for future periods used in BEM could be improved by building different scenarios of LCLU changes and following recommendations from public urban planners. Also, it is reported that the COP of AC systems decreases by 2.5–4.5% with a rise of 4 °C temperature difference between conditioned space and outdoors [61] which could lower the peak COP 9–10% for Caribbean regions and that the COP depends on the part load of the conditioned space. The uses of BEM for a constant COP are a limitation of BEM, and future work will be focused on modified BEM that accounts for dynamic COP of buildings in order to improve the results. Most of these limitations could be addressed by reliable observation records both for building parameters and AC parameters used in BEM. Also, a strong correlation was observed between minimum temperatures and AC demand [47]. Future works can rely on studying the relationship of AC ownership with mean and minimum temperatures and proposing means to reduce the demands for these conditions. Future studies should may also emphasize impacts on vulnerable populations to warmer urban environments. We hope this study serves as a template and encourages similar studies in other coastal tropical cities to plan mitigation measures for a warming climate.

Acknowledgment

The analysis process is conducted at the high-performance computing facilities at City College of New York,[4] and National Center for Atmospheric Research (NCAR), high-performance computing center.[5] The US National Science Foundation provided financial support for this research (Grant No. CBET-1438324; Funder ID: 10.13039/100000001) and CRISP (Grant No. 1832678) as well as the US Agency for International Development (Grant No. AID-517-A-15-00002; Funder ID: 10.13039/100000200).

Conflict of Interest

There are no conflicts of interest.

Data Availability Statement

The datasets generated and supporting the findings of this article are obtainable from the corresponding author upon reasonable request. Data provided by a third party are listed in Acknowledgment.

[4] http://cuerg.ccny.cuny.edu/
[5] https://cunyhpc.csi.cuny.edu/

Table 3 Urban parameters used in urban WRF simulation

		Input parameters for BEM-building parameters						
Parameters	Units	Compact H rise	Compact M rise	Compact L rise	Open H rise	Open L rise	Large L rise	Sparsely built
Urban fraction	%	100	95	90	65	65	85	30
Roof heat capacity	J/(m^3 K)	1.95×10^6	2.4×10^6	2.219×10^6	1.95×10^6	2.219×10^6	2.4×10^6	8.916×10^6
Roof thermal conductivity	W/(m K)	1.1538	0.937	0.649	1.1538	0.649	0.937	0.1615
Roof albedo	%	13 & 70	18 & 70	15 & 70	13 & 70	13 & 70	18 & 70	13 & 70
Roof emissivity	%	91	91	91	91	91	91	91
Roof width	M	15	17.5	9	32	105	28.8	10
Ground heat capacity	J/(m^3 K)	3.84×10^6	4.14×10^6	4.425×10^6	4.88×10^6	5.07×10^6	4.20×10^6	5.833×10^6
Ground thermal conductivity	W/(m K)	0.4004	0.4004	0.4004	0.4004	0.4004	0.4004	0.4004
Ground albedo	%	15	15	16	17	18	16	19
Ground emissivity	%	95	95	95	95	95	95	95
Wall heat capacity	J/(m^3 K)	1.698×10^6	4.266×10^6	3.945×10^6	2.5×10^6	3.94×10^6	2.4×10^6	15.8×10^6
Wall thermal conductivity	W/(m K)	1.1538	0.937	0.649	1.1538	0.649	0.9375	0.1615
Wall albedo	%	25	20	20	25	25	25	25
Wall emissivity	%	90	90	90	90	90	90	90
Road width	M	15	12.7	5.7	37.5	12.4	32.5	10
Building height	M	25	17.5	6.5	25	6.5	6.5	6.5
Building area fraction	%	50	40	40	20	20	20	16
Input parameters for BEM AC systems								
COP of AC system		3 & 3.5	3 & 3.5	3 & 3.5	3 & 3.5	3 & 3.5	3 & 3.5	3 & 3.5
Target indoor temperature	K	297	297	297	297	297	297	298
Comfort range of indoor temperature	K	2	2	2	2	2	2	2
Target indoor humidity	kg/kg	0.01	0.01	0.01	0.01	0.01	0.01	0.01
Comfort range of indoor humidity	kg/kg	0.002	0.002	0.002	0.002	0.002	0.002	0.002
Occupants per floor	People/m^2	0.02	0.01	0.0032	0.0032	0.001	0.01	0.00043
Initial and end times of AC systems	h	1–24	1–24	1–24	1–24	1–24	1–24	1–24
Peak heat generated by equipment	W/m^2	36	30	25	20	15	36	10
Diurnal profile of heat generated by equipment (1–24 h)		0.25, 0.25, 0.25, 0.25, 0.25, 0.25, 0.25, 0.5, 1, 1, 1, 1, 1, 1, 1, 1, 1, 0.5, 0.15, 0.25, 0.25, 0.25, 0.25						

References

[1] IEA 2018, The Future of Cooling: Opportunities for Energy-Efficient Air Conditioning (International Energy Agency). https://webstore.iea.org/the-future-of-cooling

[2] Edwards, E. E., Iyare, O. S., and Moseley, L. L., 2012, "Energy Consumption in Typical Caribbean Office Buildings: A Potential Short-Term Solution to Energy Concerns," Renew. Energy, **39**(1), pp. 154–161.

[3] Macpherson, C., and Akpinar-Elci, M., 2013, "Impacts of Climate Change on Caribbean Life," Am. J. Public Health, **103**(1), p. e6.

[4] Glenn, E., Comarazamy, D., González, J. E., and Smith, T., 2015, "Detection of Recent Regional Sea Surface Temperature Warming in the Caribbean and Surrounding Region," Geophys. Res.-Lett., **42**(16), pp. 6785–6792.

[5] Angeles-Malaspina, M., González-Cruz, J. E., and Ramírez-Beltran, N., 2018, "Projections of Heat Waves Events in the Intra-Americas Region Using Multimodel Ensemble," Adv. Meteorol., **2018**(1), p. 16.

[6] Angeles-Malaspina, M., González-Cruz, J. E., and Ramírez-Beltran, N., 2018, "Projections of Heat Waves Events in the Intra-Americas Region Using Multimodel Ensemble," Adv. Meteorol., **133**(1), pp. 59–72.

[7] Ortiz, L., González, J. E., and Lin, W., 2018, "Climate Change Impacts on Peak Building Cooling Energy Demand in a Coastal Megacity," Environ. Res. Lett., **13**(9), p. 094008.

[8] Lipson, J. M., Thatcher, M., Hart, A. M., and Pitman, A., 2019, "Climate Change Impact on Energy Demand in Building-Urban-Atmosphere Simulations Through the 21st Century," Environ. Res. Lett., **14**(12), 125014.

[9] United Nations Environment Programme (UNEP), 2003, "Climate Change in Latin America and the Caribbean: Current State and Opportunities," Proceedings of the 14th Meeting of the Forum of Ministers of the Environment of Latin America and the Caribbean, Panama, Nov. 20–25, Vol. 1, pp. 1–27.

[10] United Nations Environment Programme (UNEP), 2000, Promotion of New and Renewable Sources of Energy, Including the Implementation of the World Solar Programme 1996–2005. Report of the Secretary General-UNEP, 55th Session, Article 97f, pp. 1–7.

[11] Stoeglehner, G., Niemetz, N., and Kettl, K. H., 2011, "Spatial Dimensions of Sustainable Energy Systems: New Visions for Integrated Spatial and Energy Planning," Energy Sustain. Soc., **1**(1), pp. 1–9.

[12] Taleb, H. M., 2014, "Using Passive Cooling Strategies to Improve Thermal Performance and Reduce Energy Consumption of Residential Buildings in U.A.E. Buildings," Front. Archit. Res., **3**(2), pp. 154–165.

[13] Lucero-álvarez, J., Rodríguez-Muñoz, N. A., and Martín-Domínguez, I. R., 2016, "The Effects of Roof and Wall Insulation on the Energy Costs of Low Income Housing in Mexico," Sustainability, **8**(7), pp. 1–19.

[14] Liddament, M. W., and Orme, M., 1988, "Energy and Ventilation," Appl. Therm. Eng., **18**(11), pp. 1101–1109.

[15] Hoyt, T., Arens, E., and Zhang, H., 2014, "Extending Air Temperature Setpoints: Simulated Energy Savings and Design Considerations for New and Retrofit Buildings," Build. Environ., **88**, pp. 89–96.

[16] Rosenfeld, A. H., Akbari, H., Bretz, S., Fishman, B. L., Kurn, D. M., Sailor, D., and Taha, H., 1995, "Mitigation of Urban Heat Islands: Materials, Utility Programs, Updates," Energy Build., **22**(3), pp. 255–265.

[17] Reyna, J., and Chester, M., 2017, "Energy Efficiency to Reduce Residential Electricity and Natural Gas Use Under Climate Change," Nat. Commun., **8**(1), pp. 1–12.

[18] Wang, N., Phelan, P. E., Gonzalez, J., Harris, C., Henze, G. P., Hutchinson, R., Langevin, J., Lazarus, M. A., Nelson, B., Pyke, C., Roth, K., Rouse, D., Sawyer, K., and Selkowitz, S., 2017, "Ten Questions Concerning Future Buildings Beyond Zero Energy and Carbon Neutrality," Build. Environ., **119**, pp. 169–182.

[19] Salamanca, F., Georgescu, M., Mahalov, A., Moustaoui, M., and Martilli, A., 2016, "Citywide Impacts of Cool Roof and Rooftop Solar Photovoltaic Deployment on Near-Surface Air Temperature and Cooling Energy Demand," Boundary Layer Meteorol., **161**(1), pp. 203–221.

[20] Roman, K. K., O'Brien, T., Alvey, J. B., and Woo, O. J., 2016, "Simulating the Effects of Cool Roof and PCM (Phase Change Materials) Based Roof to Mitigate UHI (Urban Heat Island) in Prominent US Cities," Energy, **96**, pp. 103–117.

[21] Ortiz, L. E., Gonzalez, J. E., Gutierrez, E., and Arend, M., 2016, "Forecasting Building Energy Demands With a Coupled Weather-Building Energy Model in a Dense Urban Environment," ASME J. Sol. Energy Eng., **139**(1), p. 011002.

[22] Cotana, F., Rossi, F., Filipponi, M., Coccia, V., Pisello, A. L., Bonamente, E., Petrozzi, A., and Cavalaglio, G., 2014, "Albedo Control as an Effective Strategy to Tackle Global Warming: A Case Study," Appl. Energy, **130**, pp. 641–647.

[23] Oleson, K. W., Bonan, G. B., and Feddema, J., 2010, "Effects of White Roofs on Urban Temperature in a Global Climate Model," Geophys. Res. Lett., **37**(3), p. L03701.

[24] Akbari, H., Pomerantz, M., and Taha, H., 2001, "Cool Surfaces and Shade Trees to Reduce Energy Use and Improve Air Quality in Urban Areas," Sol. Energy, **70**(3), pp. 295–310.

[25] Masson, V., Bonhomme, M., Salagnac, J.-L., Briottet, X., and Lemonsu, A., 2014, "Solar Panels Reduce Both Global Warming and Urban Heat Island," Front. Environ. Sci., **2**, pp. 14.

[26] Pokhrel, R., Walker, A., and González, J. E., 2020, "A New Methodology to Assess Building Integrated Roof top PV Installations at City Scales: The Tropical Coastal City Case," ASME J. Eng. Sustain. Build. Cities, **1**(1), p. 011004.

[27] Scherba, A., 2011, "Modeling the Impact of Roof Reflectivity, Integrated Photovoltaic Panels and Green Roof Systems on the Summertime Heat Island," Dissertations and Theses. Paper 246. https://pdxscholar.library.pdx.edu/open_access_etds/246

[28] Pokhrel, R., Ramirez-Beltran, N., and González, J., 2019a, "On the Assessment of Alternatives for Building Cooling Load Reductions for a Tropical Coastal City," Energy Build., **182**, pp. 131–143.

[29] PREPA, 2019, "Integrated Resource Plan," IRP, https://energia.pr.gov/en/integrated-resource-plan/

[30] Beccali, M., Cellura, M., Lo Brano, V., and Marvuglia, A., 2004, "Forecasting Daily Urban Electric Load Profiles Using Artificial Neural Networks," Energy Convers. Manag., **45**(18–19), pp. 2879–2900.

[31] Howard, B., Parshall, L., Thompson, J., Hammer, S., Dickinson, J., and Modi, V., 2012, "Spatial Distribution of Urban Building Energy Consumption by End Use," Energy Build., **45**, pp. 141–151.

[32] Ahmed, K., Ortiz, L. E., and González, J. E., 2017, "On the Spatio-Temporal End-User Energy Demands of a Dense Urban Environment," ASME J. Sol. Energy Eng., **139**(4), p. 041005.

[33] Olivo, Y., Hamidi, A., and Ramamurthy, P., 2017, "Spatiotemporal Variability in Building Energy Use in New York City," Energy, **141**, pp. 1393–1401.

[34] Vahmani, P., Sun, F., Hall, A., and Ban-Weiss, G., 2016, "Investigating the Climate Impacts of Urbanization and the Potential for Cool Roofs to Counter Future Climate Change in Southern California," Environ. Res. Lett., **11**(12), p. 124027.

[35] Tewari, M., Salamanca, F., Martilli, A., Treinish, L., and Mahalov, A., 2017, "Impacts of Projected Urban Expansion and Global Warming on Cooling Energy Demand Over a Semiarid Region," Atmos. Sci. Lett., **18**(11), pp. 419–426.

[36] Skamarock, W. C., Klemp, J. B., Dudhia, J., Gill, D. O., Barker, D. M., Duda, M. G., Huang, X.-Y., Wang, W., and Powers, J. G., 2008, "A Description of the Advanced Research WRF Version 3," University Corporation for Atmospheric Research, Report No. NCAR/TN-475+STR.

[37] Brúyere, C., Monaghan, A., Steinhoff, D., and Yates, D., 2015, Bias-Corrected CMIP5 CESM Data in WRF/MPAS Intermediate File Format (UCAR/NCAR) NCAR Technical Note NCAR/TN-515+STR.

[38] Bruyère, C. L., Done, J. M., Holland, G. J., and Fredrick, S., 2014, "Bias Corrections of Global Models for Regional Climate Simulations of High-Impact Weather," Clim. Dyn., **43**(7–8), pp. 1847–1856.

[39] Ching, J., Brown, M., Burian, S., Chen, F., Cionco, R., Hanna, A., Hultgren, T., McPherson, T., Sailor, D., Taha, H., and Williams, D., 2009, "National Urban Database and Access Portal Tool," Bull. Am. Meteorol. Soc., **90**(8), pp. 1157–1168.

[40] Stewart, I. D., and Oke, T. R., 2012, "Supplement Datasheets for Local Climate Zones," Bull. Am. Meteorol. Soc., **92**, pp. 108–125.

[41] Tewari, M., Chen, F., Wang, W., Dudhiav, J., LeMone, M., Mitchell, K., Ek, M., Gayno, G., Wegiel, J., and Cuenca, R., 2004, "Implementation and Verification of the Unified NOAH Land Surface Model in the WRF Model," 20th Conference on Weather Analysis and Forecasting/16th Conference on Numerical Weather Prediction, Seattle, WA, Jan. 10–15, pp. 11–15.

[42] Kain, J. S., 2004, "The Kain–Fritsch Convective Parameterization: An Update," J. Appl. Meteorol., **43**(1), pp. 170–181.

[43] Hong, S., and Lim, J., 2006, "The WRF Single-Moment 6-Class Microphysics Scheme (WSM6)," J. Korean Meteorol. Soc., **42**(2), pp. 129–151.

[44] Martilli, A., Clappier, A., and Rotach, M. W., 2002, "An Urban Surface Exchange Parameterisation for Mesoscale Models," Boundary-Layer Meteorol., **104**(2), pp. 261–304.

[45] Salamanca, F., and Martilli, A., 2010, "A New Building Energy Model Coupled With an Urban Canopy Parameterization for Urban Climate Simulations-Part II. Validation With One Dimension Off-Line Simulations," Theor. Appl. Climatol., **99**(3–4), pp. 345–356.

[46] Dudhia, J., 1989, "numerical Study of Convection Observed During the Winter Monsoon Experiment Using a Mesoscale Two-Dimensional Model," J. Atmos. Sci., **46**(20), pp. 3077–3107.

[47] Mlawer, E. J., Taubman, S. J., Brown, P. D., Iacono, M. J., and Clough, S. A., 1997, "Radiative Transfer for Inhomogeneous Atmospheres: RRTM, a Validated Correlated-k Model for the Longwave," J. Geophys. Res. Atmos., **102**(D14), pp. 16663–16682.

[48] Janjic, Z. I., 2002, "Nonsingular Implementation of the Mellor-Yamada Level 2. 5 Scheme in the NCEP Meso Model," National Centers for Environmental Prediction, p. 61.

[49] Pokhrel, R., Ortiz, L. E., Ramírez-Beltran, N. D., and González, J. E., 2019b, "On the Climate Variability and Energy Demands for Indoor Human Comfort Levels in a Tropical-Coastal Urban Environment," ASME J. Sol. Energy Eng., **141**(3), p. 031002.

[50] van Vuuren, D. P., Edmonds, J., Kainuma, M., Riahi, K., Thomson, A., Hibbard, K., Hurtt, G. C., Kram, T., Krey, V., Lamarque, J.-F., Masui, T., Meinshausen, M., Nakicenovic, N., Smith, S. J., and Rose, S. K., 2011, "The Representative Concentration Pathways: An Overview," Clim. Change, **109**(1–2), pp. 5–31.

[51] ASHRAE, 1999, "HVAC Application Handbook," Handbook.

[52] Gutiérrez, E., González, J. E., Bornstein, R., Arend, M., and Martilli, A., 2013, "A New Modeling Approach to Forecast Building Energy Demands During Extreme Heat Events in Complex Cities," ASME J. Sol. Energy Eng., **135**(4). p. 040906.

[53] Stewart, I. D., Oke, T. R., and Krayenhoff, E. S., 2014, "Evaluation of the 'Local Climate Zone' Scheme Using Temperature Observations and Model Simulations," Int. J. Climatol., **34**(4), pp. 1062–1080.

[54] Méndez-Lázaro, P., Martínez-Sánchez, O., Méndez-Tejeda, R., Rodríguez, E., and Morales, E., 2015, "Extreme Heat Events in San Juan Puerto Rico:

Trends and Variability of Unusual Hot Weather and Its Possible Effects on Ecology," J. Climat. Weath. Forecast., **3**(2), pp. 1000135-1–1000135-7.
[55] Reddy, T. A., Kreider, J. F., Curtiss, P. S., and Rabl, A., 2016, *Heating and Cooling of Buildings: Principles and Practice of Energy Efficient Design*, CRC Press, Taylor & Francis Group, UK.
[56] Ohashi, Y., Genchi, Y., Kondo, H., Kikegawa, Y., Yoshikado, H., and Hirano, Y., 2007, "Influence of Air-Conditioning Waste Heat on Air Temperature in Tokyo During Summer: Numerical Experiments Using an Urban Canopy Model Coupled With a Building Energy Model," J. Appl. Meteorol., **46**(1), pp. 66–81.
[57] Izquierdo, M., Moreno-Rodriguez, A., Gonzalez-Gil, A., and Garcia-Hernando, N., 2011, "Air Conditioning in the Region of Madrid, Spain: An Approach to Electricity Consumption, Economics and CO_2 Emissions," Energy, **36**(3), pp. 1630–1639.
[58] Salamanca, F., Georgescu, M., Mahalov, A., Moustaoui, M., Wang, M., and Svoma, B. M., 2013, "Assessing Summertime Urban Air Conditioning Consumption in a Semiarid Environment," Environ. Res. Lett., **8**(3), p. 034022.
[59] Xu, X., Chen, F., Shen, S., Miao, S., Barlage, M., Guo, W., and Mahalov, A., 2018, "Using WRF-Urban to Assess Summertime Air Conditioning Electric Loads and Their Impacts on Urban Weather in Beijing," JGR Atmos., **123**(5), pp. 2475–2490.
[60] Sailor, D. J., and Pavlova, A. A., 2003, "Air Conditioning Market Saturation and Long-Term Response of Residential Cooling Energy Demand to Climate Change," Energy, **28**(9), pp. 941–951.
[61] Jongmin, C., and Yongchan, K., 2002, "The Effects of Improper Refrigerant Charge on the Performance of a Heat Pump With an Electronic Expansion Valve and Capillary Tube," Energy, **27**(391), pp. 391–404.